

RedoXplore

Official Journal of the Serbian Society for Mitochondrial and Free Radical Physiology





Research Article

Mitochondrial Sirt3 in Kidney Aging: Sex-Specific Links to Metabolic Homeostasis and Oxidative Stress

Ena Simunic^{1,a}, Kate Seselja^{1,a}, Iva I. Podgorski¹, Marija Pinteric¹, Robert Beluzic¹, Marijana Popovic Hadzija¹, Tihomir Balog¹, Hansjörg Habisch², Tobias Madl³, Sandra Sobocanec^{1,*}

Keywords

Sirtuin 3 Sex differences Murine kidney Aging Oxidative stress

Abstract

Aging is a complex biological process that begins at the cellular level, disrupting energy homeostasis. The mitochondrial deacetylase Sirtuin 3 (Sirt3) plays a key role in maintaining this balance by deacetylating proteins involved in metabolic pathways essential for energy production. This study investigated the role of Sirt3 in sex-dependent changes in energy homeostasis during aging using an *in vivo* mouse model. The findings emphasize the sex-specific function of Sirt3 in regulating mitochondrial activity, energy metabolism, and oxidative stress in the murine kidney, with male mice exhibiting a greater reliance on Sirt3 for metabolic stability. Higher Sirt3 expression in male WT mice leads to increased vulnerability to its deficiency, as reflected in the shorter lifespan of male KO mice. This is further supported by distinct metabolomic clustering in male KO mice, highlighting significant metabolic disruptions. Male-specific declines in metabolites such as creatine, phosphorylcholine, trimethylamine-N-oxide, and L-carnitine, along with reduced trifunctional multienzyme complex subunit β (HADHB) expression, point to impaired fatty acid metabolism and mitochondrial dysfunction.

Introduction

The aging of multicellular organisms is a complex biological process that is accompanied by a progressive deterioration in the functions of most organs. The changes that occur during aging start at the cellular level, including the accumulation of DNA damage, telomere shortening, alterations in the cell cycle, mitochondrial dysfunction, epigenetic modi-

fications, and the buildup of misfolded proteins, all of which collectively disrupt energy homeostasis¹. There are considerable individual and sex-specific differences in the aging process. In humans, many age-related diseases manifest differently depending on sex. It is known that in mammals, females live longer than males and are in poorer health towards the end of their lives².

DOI: https://doi.org/10.70200/RX202501001S

Received: 10 July 2025; Revised: 2 August 2025; Accepted: 10 September 2025.

Published by Opus Journal. This is an open access article under the CC BY-NC-ND 4.0 license (https://creativecommons.org/licenses/by-nc-sa/4.0/).

¹ Division for Molecular Medicine, Rudjer Boskovic Institute, Zagreb 10 000, Croatia

² Division of Medicinal Chemistry, Medical University of Graz, Graz 8010, Austria

³ BioTechMed Graz, Graz 8010, Austria

^{*} Corresponding author. Division for Molecular Medicine, Rudjer Boskovic Institute, Bijenicka cesta 54, 10 000 Zagreb, Croatia. E-mail address: ssoboc@irb.hr

^a These authors contributed equally to this work.

One of the main hallmarks of aging is mitochondrial dysfunction, which leads to impaired energy homeostasis and increased production of reactive oxygen species (ROS). Sirtuin 3 (Sirt3) is the major mitochondrial deacetylase belonging to the sirtuin family, an evolutionary highly conserved group of enzymes whose main function is the deacetylation of lysine residues in numerous proteins³. Sirt3 plays an important role in the regulation of energy metabolism, as the function of many proteins involved in energy production pathways is regulated by Sirt34. Numerous studies have shown that the absence of Sirt3 leads to impaired mitochondrial function⁵. As mitochondrial superoxide dismutase (SOD) is a known target of Sirt3, deficient deacetylation can also lead to increased oxidative stress in the cell6. Considering the sex-specific differences in mitochondria, an important question emerges regarding the distinct role of Sirt3 in each sex.

The kidneys play a crucial role in maintaining metabolic balance and energy homeostasis by regulating nutrient levels, glucose production and hormonal activity. They regulate energy metabolism by reabsorbing essential nutrients such as glucose and amino acids during urine formation, thus conserving energy resources. They also modulate lipid and protein metabolism by filtering and metabolising circulating molecules such as fatty acids and peptides7. Sirtuins are expressed in the different renal compartments and it is likely that Sirt3 plays an important role in the regulation of metabolic functions in the kidney8. There is evidence that the activity of Sirt3 in the kidney correlates with the maintenance of mitochondrial energy homeostasis and antioxidant defence. Sirt3 has also been shown to be a key regulator of mitochondrial dynamics in kidney cells9. Furthermore, recently some research has been done on the role of Sirt3 in renal diseases¹⁰, but there is limited information on the sex-specific role of the Sirt3 in the context of renal aging.

The aim of this study was to investigate the role of Sirt3 in sex-specific changes in energy homeostasis during aging in mouse kidney. Renal lipid peroxidation, protein carbonylation, relative protein expression, and the activities of antioxidant enzymes were analysed, along with metabolomic profiling. Understanding the role of Sirt3 in sex-specific metabolic regulation could provide relevant knowledge for the development of targeted therapies, emphasizing the importance of considering sex differences in metabolic research.

Materials & Methods

Animal model

Wild-type (WT, Sirt3+/+, Stock No.: 002448) and Sirt3 knockout (KO, Sirt3-/-, Stock No.: 012755) 129S1/ SvImJ mice of both sexes (Jackson Laboratory, Bar Harbor, ME, USA) were housed under standard conditions (three mice per cage, 22°C, 50–70% humidity and a 12-hour light cycle). The animals were divided into eight groups, with six mice per group: WT males, KO males, WT females and KO females were sacrificed at 4 months of age, and WT males, KO males, WT females and KO females were sacrificed at 14 months of age. An additional four groups, each consisting of eight mice (WT males, KO males, WT females, and KO females), were monitored until natural death to generate survival curves. Body weight and glucose levels were measured once a week. Before the glucose measurements, the mice were fasted for 6 h. After 4 and 14 months, the mice were anaesthetised with an intraperitoneal injection of ketamine/xylazine, sacrificed and the tissues were stored in liquid nitrogen until analysis.

Tissue homogenization

To measure SOD and catalase activity, protein carbonylation and lipid peroxidation, a 10% kidney homogenate was prepared in PBS with cOmplete™, EDTA-free protease inhibitor cocktail tablets (Roche, Basel, Switzerland) using a Braun Potter S homogeniser (Labexchange, Germany) (1300 rpm, 1 min). The samples were then sonicated 3 x 30 s (amplitude 80%), centrifuged for 15 min at 16,000 g and 4°C and supernatants were transferred to new tubes. For Western blot analysis, the homogenates were prepared in RIPA buffer with cOmplete™, EDTA-free protease inhibitor cocktail tablets (Roche, Basel, Switzerland), following the same protocol.

Superoxide dismutase (SOD) and catalase activity

For SOD and catalase activity measurement, the protein concentration in kidney homogenates was measured in PBS using the Pierce™ BCA Protein Assay Kit (Thermo Fischer Scientific, USA). Samples were diluted to 0.05 mg/mL for measurement of total SOD activity and 0,5 mg/mL for MnSOD activity. A RANSOD kit (Randox Laboratories, UK) was used for activity measurement according to the manufacturer's instructions. Absorbance was measured us-

ing a Tecan Infinite 200 spectrophotometer (Tecan Group Ltd, Switzerland) at 505 nm. Enzyme activity was normalised to the protein concentration in each sample.

The Catalase activity was measured, with slight modifications, as previously described¹¹, by measuring the change in absorbance (at 240 nm) in the reaction mixture during the interval of 30 s following sample addition. The kidney samples were diluted 500x in 50 mM PBS (pH 7.0) and the final concentration of 10 mM H₂O₂ was used. Change in absorbance was measured at 240 nm using an Ultrospec 2100 pro spectrophotometer (Amersham Biosciences, USA).

Lipid peroxidation

TBARS (thiobarbituric acid reactive substances) analysis was used to measure the amount of lipid peroxides. The main product of lipid peroxidation is malondialdehyde (MDA), which reacts with 2-thiobarbituric acid (TBA) to form a measurable fluorescent adduct. 150 μ L of the previously prepared kidney homogenates were transferred to Eppendorf tubes. 1,1,3,3-tetramethoxypropane (TMP) standards were prepared by diluting 100 mM stock solution (prepared by mixing 1.66 μ L TMP and 98.34 μ L 96% ethanol). TMP hydrolyses to MDA, which enables the preparation of the standard curve.

As with the samples, 150 µL of the standard was transferred to Eppendorf tubes. 150 µL of 2% SDS was added to the standards and samples, mixed with a vortex and incubated for 5 min at room temperature. Then 375 µL of a 28.5 mM solution of 2-thiobarbituric acid (TBA), pH 3.5, was added and the samples were incubated for 1 h at 95°C in a thermomixer. After brief cooling, the samples were centrifuged at 4000 g for 10 min at room temperature. 200 µL of each sample and standard were transferred in duplicate to a black 96-well plate. Fluorescence was measured using a Tecan Infinite 200 spectrophotometer (Tecan Group Ltd, Switzerland) at 520/550 nm (excitation/emission). The MDA concentration in the samples was calculated from the obtained standard curve and normalised to the protein concentration in the individual sample.

Protein Carbonylation

To measure protein carbonylation, the protein concentration was measured using the PierceTM BCA Protein Assay Kit (Thermo Fischer Scientific, USA) and 10 μ g/mL solutions were prepared for each sample. 100

µL of the prepared solutions were plated in triplicate onto a Nunc™ MaxiSorp™ (Thermo Fisher Scientific, USA) 96-well plate and incubated overnight at 4°C. The next day, the wells were washed twice with PBS and 200 µL of 0.06 mM DNP derivatisation solution was added (a 0.1 mM stock solution was prepared by dissolving 20 mg of 2,4-dinitrophenylhydrazine (DNPH) in 1 mL of trifluoroacetic acid (TFA)). The plate was incubated for 45 min in the dark at room temperature. The DNP derivatisation solution was then removed and the wells were washed three times with wash buffer II (PBS + 96% EtOH (1:1)) and three more times with PBS. 250 µL of I-Block™ Protein-Based Blocking Reagent (Invitrogen, USA) was added to the wells and the plate was incubated for 1 h at room temperature with shaking (300 rpm). After blocking, the wells were washed with wash buffer III (PBS with 0,1% Tween) and 100 µL of the prepared primary anti-DNP antibody solution (Sigma-Aldrich, D9656, dilution 1:1000) was added in blocking buffer. The plate was incubated for 2 h at room temperature with shaking (300 rpm). The wells were then washed four times with wash buffer III and 100 µL of the prepared secondary anti-rabbit antibody solution (Bio-Rad, 1706515, dilution 1:2000) was added in blocking buffer. The plate was incubated again for 1 h at room temperature with shaking (300 rpm) followed by four additional washes with wash buffer III. Then, 100 μL of a 3, 3′, 5, 5′-tetramethylbenzidine (TMB, Thermo Fischer Scientific, USA) solution was added to the wells and the onset of blue colouration was observed. Finally, 100 μ L of 0.3 M H_2SO_4 was added to stop the reaction. The absorbance at 450 nm was measured with a Multiskan EX spectrophotometer (Thermo Labsystems, Austria).

Protein isolation and Western blot analysis

Proteins were isolated from prepared kidney homogenates in RIPA buffer supplemented with cOmplete[™], EDTA-free protease inhibitor cocktail tablets (Roche, Basel, Switzerland). After centrifugation, the supernatant was transferred to new tubes and the protein concentration was measured using the Pierce[™] BCA Protein Assay Kit (Thermo Fischer Scientific, USA).

The proteins (15 μg/20 μL) were resolved by SDS-PAGE and transferred to a PVDF membrane (Roche, Basel, Switzerland). The membranes were blocked with I-BlockTM Protein-Based Blocking Reagent (Invitrogen, USA) and incubated with primary antibodies (**Table 1**) overnight at 4°C and with the correspond-

ing secondary antibody for 1 h at room temperature. A chemiluminescence kit (Bio-Rad, Hercules, CA, USA) and the Alliance 4.7 Imaging System (UVITEC, Cambridge, UK) were used for signal detection. Amido Black dye was used to control the uniform application of the samples and to normalise the amount of protein.

Given the large number of tissue samples, a control (C) was prepared by mixing equal proportions of protein samples isolated from WT males (N=4) and applied to each SDS-PAGE gel so that all samples could be compared with each other.

Table 1. List of used antibodies.

Name	Manufacturer and catalog number		
HADHB	Santa Cruz Biotechnology, sc-271496		
Catalase	Santa Cruz Biotechnology, sc-34284		
Sirt3	Cell Signaling Technology, 5490S		
SOD2	Proteintech Group, 66474-1-lg		
PGC1α	Cell Signaling Technology, 2178S		
Secondary antibody anti-rabbit	Bio-Rad, 1706515		
Secondary antibody anti-mouse	Bio-Rad, 1706516		

sequence was used to acquire 1H 1D NMR spectra with presaturation to suppress water (cpmgpr1d, 128 scans, 73728 points in F1, 12019.230 Hz spectral width, cycle delay 4 s). The NMR spectra were then imported into Matlab2014b and analysed using a previously described script¹². TMSP was used as an internal standard for chemical shift referencing. The regions around the water, TMSP and methanol signals were excluded. Finally, the NMR spectra were aligned and a probabilistic quotient normalisation was performed¹³. Quantification of the metabolites was performed by signal integration of

the normalised spectra. For each metabolite, a representative peak without overlapping signals was identified, the start and end points of the integration were chosen to circle around this peak, and the area of the peak was integrated by summing the value for each point. Peak identification was performed using Chenomx NMR Suite 8.4 (Chenomx Inc., Edmonton, AB, Canada), the Human Metabolome Database (HMDB)¹⁴ and reference chemicals. The results were analysed using PCA and PLS-DA in MetaboAnalyst 5.0 and 6.0.

Metabolomics

In collaboration with the Medical University of Graz, tissue samples were prepared for metabolomic analysis using nuclear magnetic resonance (NMR). The kidney samples were transferred to homogenisation tubes with Precellys beads (1.4 mm zirconium oxide beads). The samples were then homogenised in a Precellys homogeniser for 2 x 20 s. After homogenisation, the samples were transferred to standard Eppendorf tubes and stored at -20°C for at least 30 min. The samples were then centrifuged at 10.000 rpm at 4°C for 30 min, and the supernatant was transferred to new tubes. The supernatant was then lyophilized for 10 h at <1 Torr, 850 rpm, 25°C in a vacuum drying chamber (Savant Speedvac SPD210) with an associated refrigeration unit (Savant RVT450) and vacuum pump (VLP120). For the NMR experiments, the samples were redissolved in 500 µL NMR buffer (0.08 M Na₂HPO₄, 4,6 mM TMSP (3-(trimethylsilyl) propionic acid-2,2,3,3-d₄ sodium salt), 0.04 (w/v) % NaN₃ in D₂O, pH adjusted to 7,4 with 8 M HCl or 5 M NaOH, respectively). The metabolic-profiling analysis was conducted at 310 K using a Bruker Avance Neo 600 MHz NMR spectrometer equipped with a TXI probe head. The Carr-Purcell-Meiboom-Gill (CPMG) pulse

Statistical analysis

SPSS Statistics 23.0 (IBM, USA) was used for statistical data processing. Before performing the analyses, the normality of the sample distribution was checked using the Shapiro-Wilk test. For normally distributed samples, a three-way ANOVA was performed to analyse the interaction effect of sex, genotype and age. In cases where a significant three-way interaction was found, simple two-way interactions and simple pairwise comparisons were tested using the Bonferroni correction. For experiments where repeated measures were performed, repeated measures twoway ANOVA was used. For data that did not follow a normal distribution, the Kruskal-Wallis test followed by Dunn's test for independent samples was used. GraphPad Prism 9.0 (GraphPad Software, USA) was used to create graphical representations. In all graphs, the effect of age is indicated by "#", the effect of genotype by "+" and the effect of sex by "*". Results with p < 0.05 were considered significant. The tables below the graphs show the p-values for each variable analysed and its interaction effect, and the symbols in the graphs indicate the results of the pairwise comparisons.

Results

Loss of Sirt3 shortens the lifespan of male mice

To analyse the effects of Sirt3 loss on lifespan, a survival analysis was performed. Four groups of mice

(Fig. 1A, B). No differences in lifespan were observed between KO males and KO females, nor between WT males and WT females, indicating that the observed effects of Sirt3 loss are male-specific rather than due to inherent sex-based differences in WT mice.

Body weight and blood glucose concentration were monitored for three months before the animals

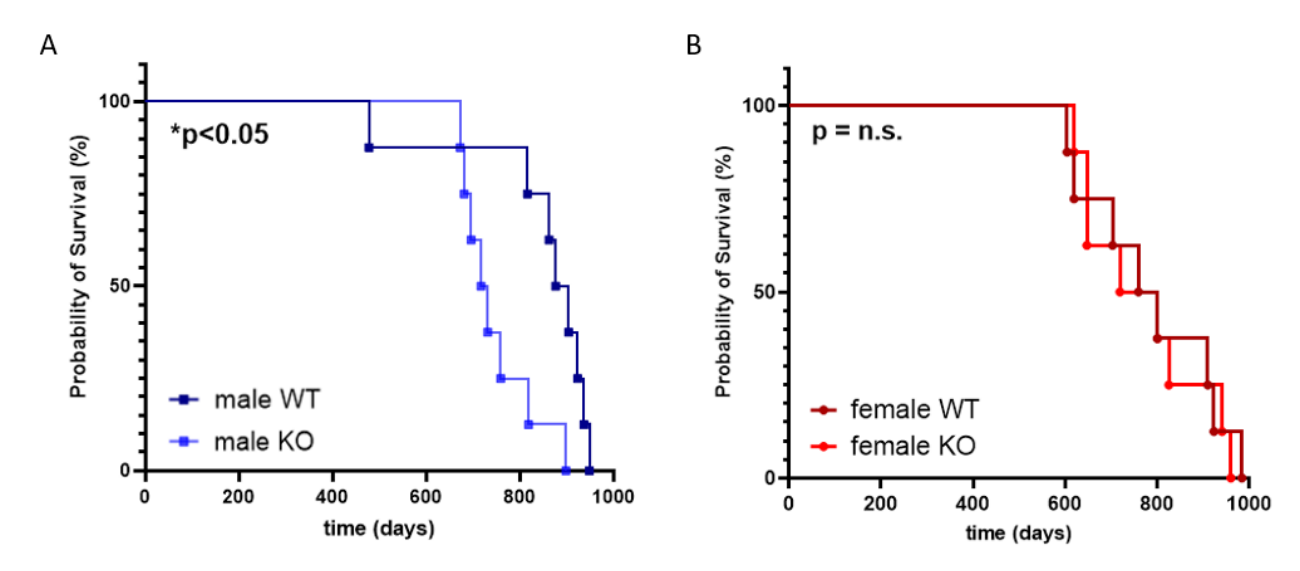


Figure 1. Sex-specific impact of Sirt3 on lifespan. Survival curve of (A) WT and KO males, (B) WT and KO females. The effect of the genotype on the survival of the mice was analysed using the Mantel-Cox test. *p<0.05, male WT vs. male KO. N=8 samples per group.

were monitored until their natural death and a survival curve was constructed (**Figure 1**).

Results of our survival analysis in vivo showed that Sirt3 KO males had a shortened lifespan compared to WT (log-rank test, $\chi 2=6.311$, p < 0.05), in contrast to females, which showed no differences in Sirt3-dependent survival (log-rank test, $\chi 2=0.028$, p = 0.866)

were sacrificed. **Figure 2** shows the trend of body weight change in young mice sacrificed at 4 months of age (**Figure 2A**) and in older mice sacrificed at 14 months of age (**Figure 2B**).

In four month old mice, both WT and KO females weighed less than their male counterparts. In older

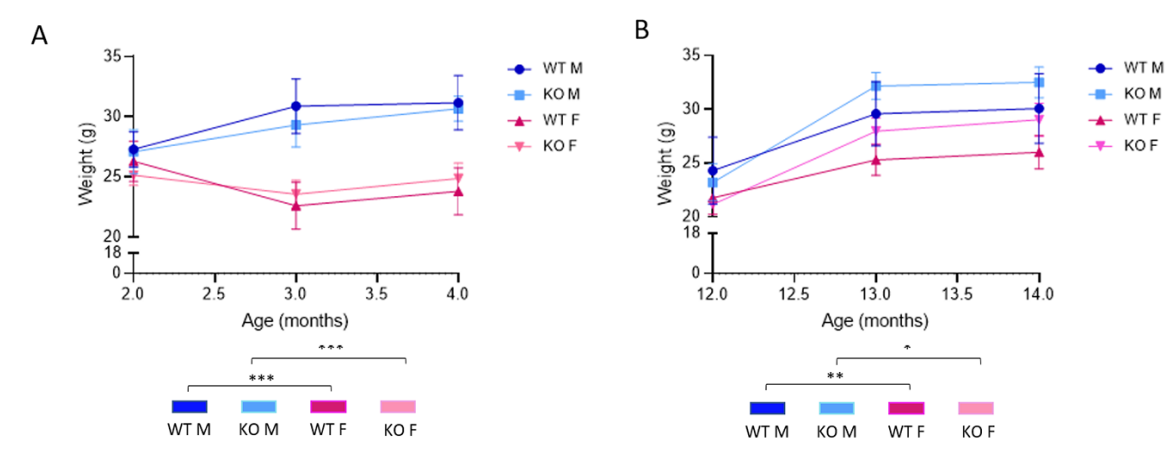


Figure 2. Weight of the mice observed over three months. The trend in weight change in each group is shown graphically. Below the graph is a legend indicating the statistical significance between the groups. (A) Mice aged 4 months, (B) mice aged 14 months. A two-way repeated measures ANOVA was performed to examine the joint effect of sex and genotype on animal weight. Simple pairwise comparisons were tested using Bonferroni correction. ***p<0.001, *p<0.05, males vs. females. Data are shown as mean ± SD. N=6 samples per group.

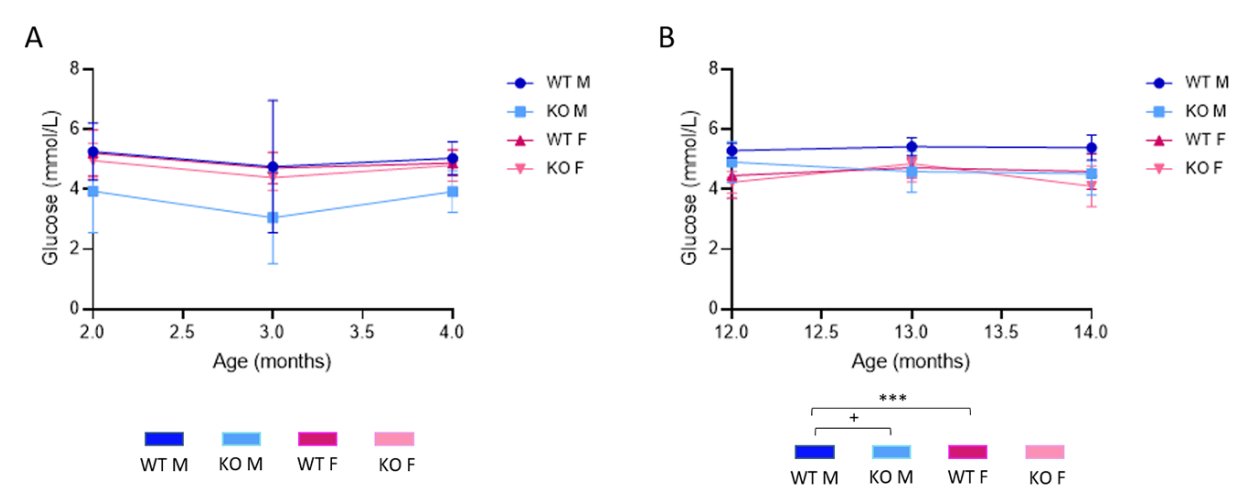


Figure 3. The blood glucose concentration of mice was monitored over a period of three months. The trend of change in blood glucose concentration in each group is shown graphically, and below the graph is a legend labelling the statistical significance between the groups. (A) Mice aged 4 months, (B) mice aged 14 months. A two-way repeated measures ANOVA was performed to examine the joint effect of sex and genotype on blood glucose levels. Simple pairwise comparisons were tested using Bonferroni correction. $^+p<0.05$, WT vs. KO, $^{***}p<0.001$, males vs. females. Data are shown as mean \pm SD. N=6 samples per group.

mice, females continued to weigh less than males, though the difference was less pronounced.

Figure 3 shows the trend of the animals' blood glucose levels. In young mice, no statistically significant differences were observed between the groups

(**Figure 3A**), while in older mice, KO males had lower blood glucose levels compared to WT males. It was also observed that WT females had lower blood glucose concentrations compared to WT males (**Figure 3B**).

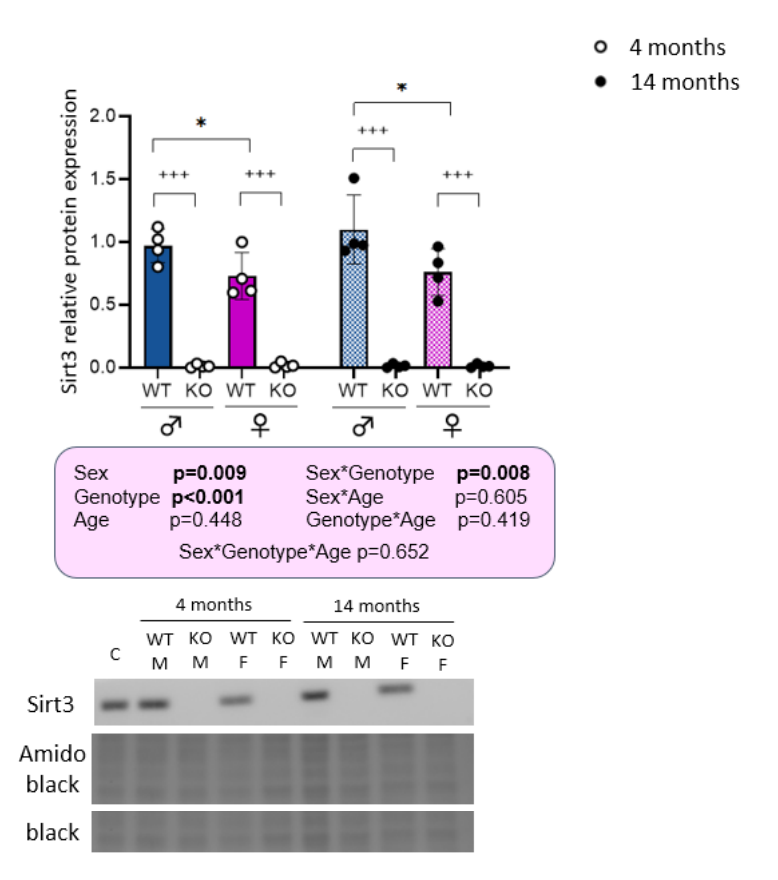


Figure 4. Relative protein expression and representative immunoblots of Sirt3 protein expression in the kidney. Amido black dye was used to control the uniform application of the samples and to normalise the amount of protein. A three-way ANOVA followed by simple pairwise comparisons with Bonferroni correction was used to examine the effects of sex, genotype and treatment. ***p<0.001, WT vs. KO, *p<0.05, males vs. females. Data are shown as mean ± SD. N=3-4 samples per group.

Sirt3 expression is higher in the kidneys of males compared to females

Western blot analysis was performed to confirm that Sirt3 expression is indeed absent in kidney tissue samples isolated from KO mice and to test whether there are sex and age-specific differences in expression. Representative immunoblots and densitometric plots of protein expression are shown in **Figure 4**. It is evident that the expression of Sirt3 is not present in renal tissue from KO mice. Moreover, the expression of Sirt3 is higher in males than females in both young and aged mice, again indicating a sexspecific role of Sirt3 in the mice kidney.

Protein expression and activity of ROS-scavenging enzymes

Since Sirt3 is known to regulate ROS scavenging, the activities of copper-zinc superoxide dismutase (CuZnSOD, SOD1), manganese superoxide dismutase (MnSOD, SOD2) and catalase were measured in the prepared kidney tissue supernatants, as well as the relative protein expression of MnSOD and catalase (**Figures 5 and 6**).

When measuring the activities of CuZnSOD and MnSOD as well as the relative protein expression of MnSOD in the kidney tissue, no statistically significant differences were found between the groups (**Figure 5**).

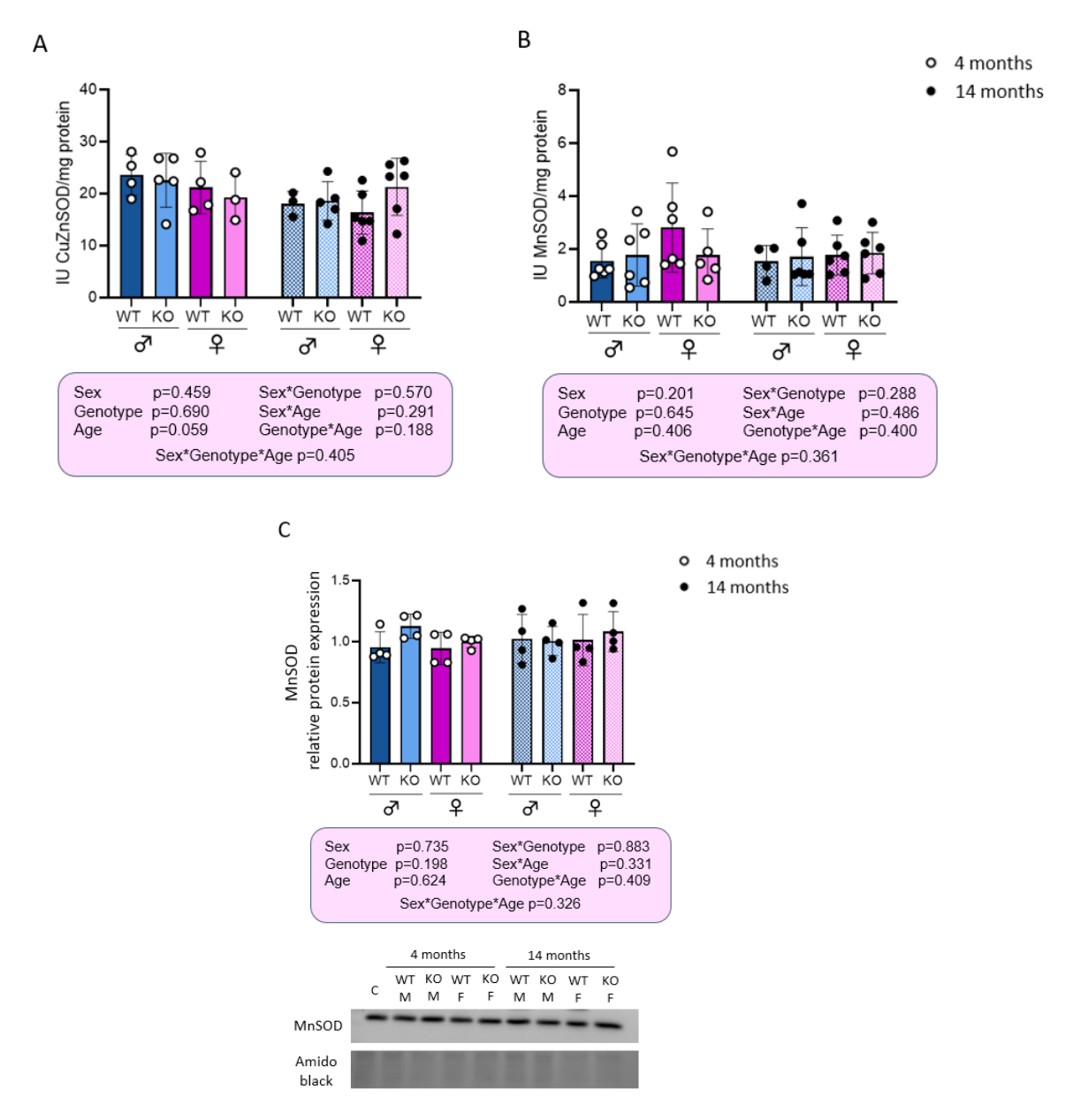


Figure 5. Activity of (A) CuZnSOD and (B) MnSOD in the kidney. (C) Relative protein expression and representative immunoblots of MnSOD protein expression in the kidney. A three-way ANOVA followed by simple pairwise comparisons with Bonferroni correction was used to examine the effect of sex, genotype and treatment. Data are shown as mean \pm SD. N=3-6 samples per group.

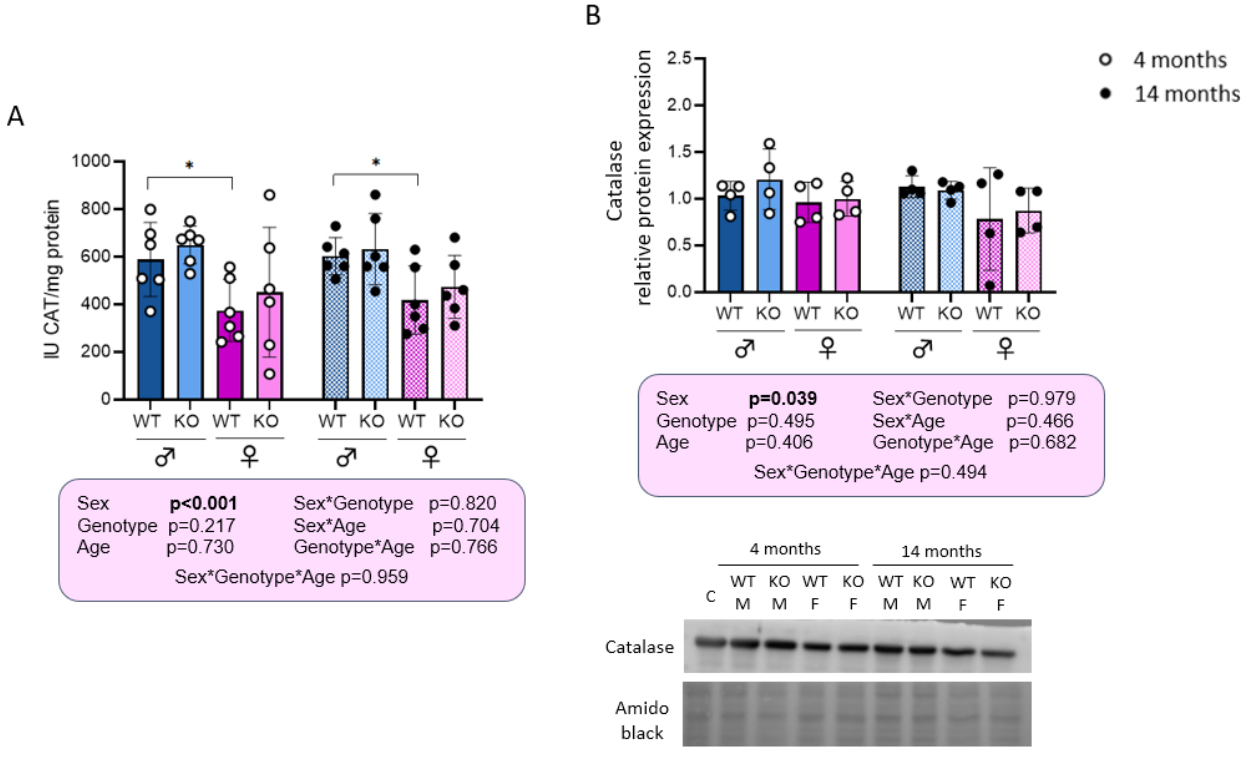


Figure 6. (A) Catalase activity in the kidney. (B) Relative protein expression and representative immunoblots of catalase expression in the kidney. A three-way ANOVA was used to analyse the interaction effect of sex, genotype and age. Simple pairwise comparisons were tested using Bonferroni correction. *p<0.05, males vs. females. Data are shown as mean \pm SD. N=3-6 samples per group.

Reduced catalase activity was observed in WT females in both age groups of mice. However, analysis of relative protein expression revealed no statistically significant differences between the groups (**Figure 6**).

The absence of Sirt3 leads to increased protein carbonylation levels in young mice

To analyse the oxidative tissue damage, the concentration of lipid peroxides and protein carbonylation were measured (**Figure 7**).

A trend towards increasing lipid peroxide concentrations was generally observed in female animals. This is particularly pronounced in older mice, where KO females show an increased concentration of lipid peroxides compared to KO males (**Figure 7A**).

Analysis of protein carbonylation levels in the kidney revealed an interaction effect between genotype and age of the animals, with Sirt3 deficiency leading to increased carbonylation levels in young mice, whereas this effect was not observed in older animals. In particular, a decrease in protein carbonylation levels were observed in aged KO females. In

addition, a trend towards a decrease in protein carbonylation was observed in females compared to males (**Figure 7B**).

Male mice have lower HADHB expression than female mice

As Sirt3 is an important regulator of mitochondrial function and energy metabolism, the expression levels of selected metabolic and mitochondrial proteins were analysed to gain an insight into the metabolic state and energy status of the organism. The subunit of the multienzyme complex for the β -oxidation of fatty acids (HADHB), was selected for its crucial role in mitochondrial fatty acid oxidation, contributing to kidney metabolic homeostasis (**Figure 8A**). Peroxisome proliferator-activated receptor gamma coactivator 1- α (PGC1 α), a mitochondrial master regulator, was selected as a representative of the mitochondrial proteins (**Figure 8B**). Its expression level can be correlated with the state of the mitochondria in the analysed samples.

Males generally have a lower expression of HADHB compared to females, and this difference is most pronounced in young mice (**Figure 8A**). On

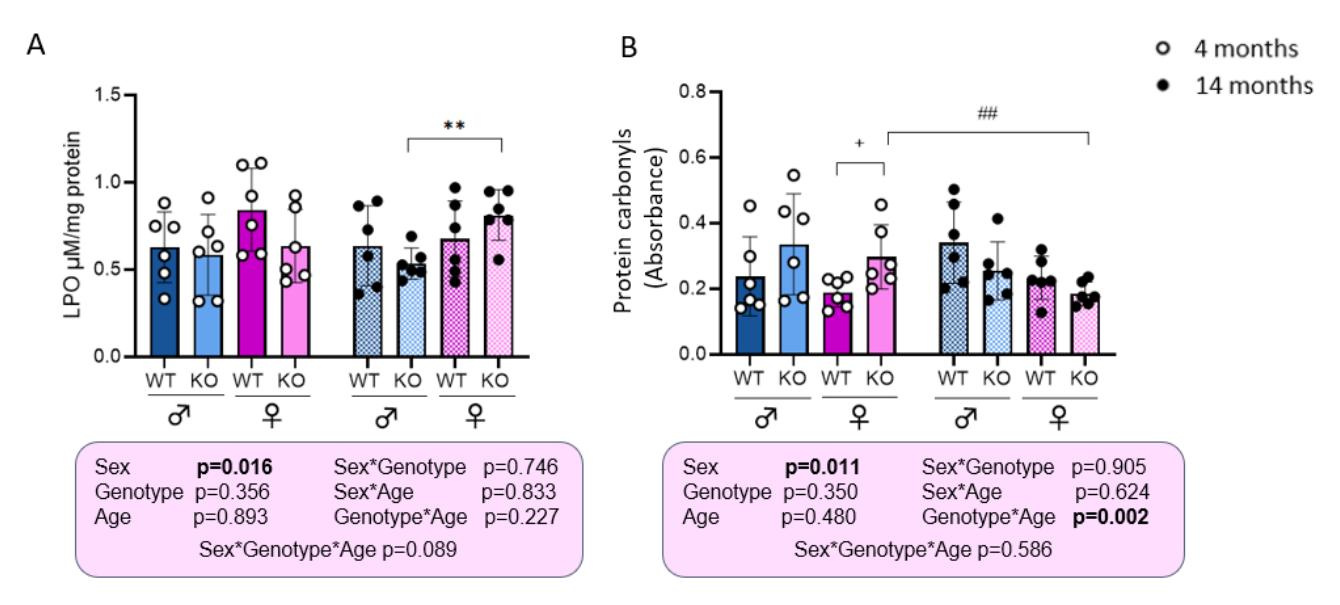


Figure 7. (A) Lipid peroxide concentrations and (B) absorbance value at 450 nm corresponding to the amount of carbonyl groups in the kidney samples. A three-way ANOVA was used to examine the interaction effect of sex, genotype and treatment. Simple pairwise comparisons were tested using Bonferroni correction. $^+p<0.05$, WT vs. KO, $^{**}p<0.01$, males vs. females, $^{\#}p<0.01$, 4 month old vs. 14 month old mice. Data are shown as mean \pm SD. N=5-6 samples per group.

the other hand, a trend towards lower expression of PGC1 α was generally observed in females, with the difference being most pronounced in KO females (**Figure 8B**).

Metabolic profiling reveals sex-specific differences

Metabolomic analysis of kidney tissue from 4 and 14 month old mice was performed using NMR. PLS-DA analysis was performed separately for tissue sam-

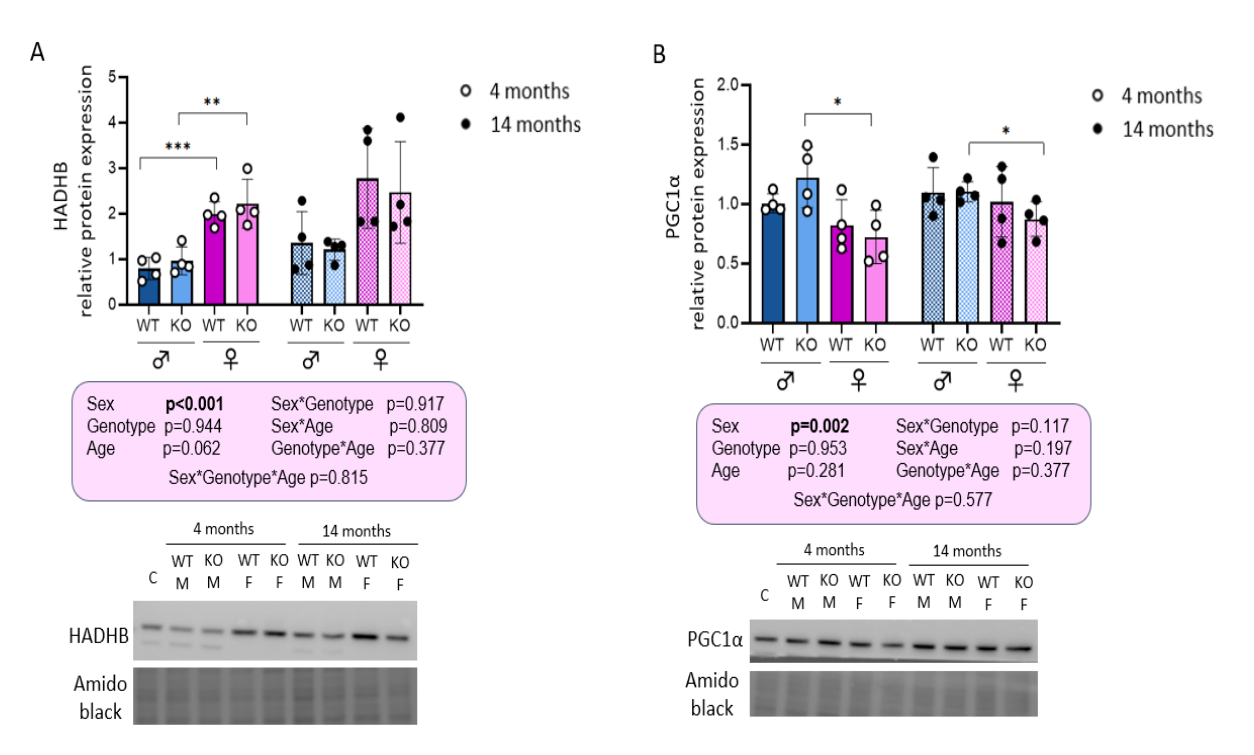


Figure 8. Relative protein expression and representative immunoblots of (A) HADHB and (B) PGC1 α in the kidney. A three-way ANOVA was used to examine the interaction effect of sex, genotype and treatment. Simple pairwise comparisons were tested using Bonferroni correction. ***p<0.001, **p<0.01 males vs. females. Data are expressed as mean \pm SD. N=4 samples per group.

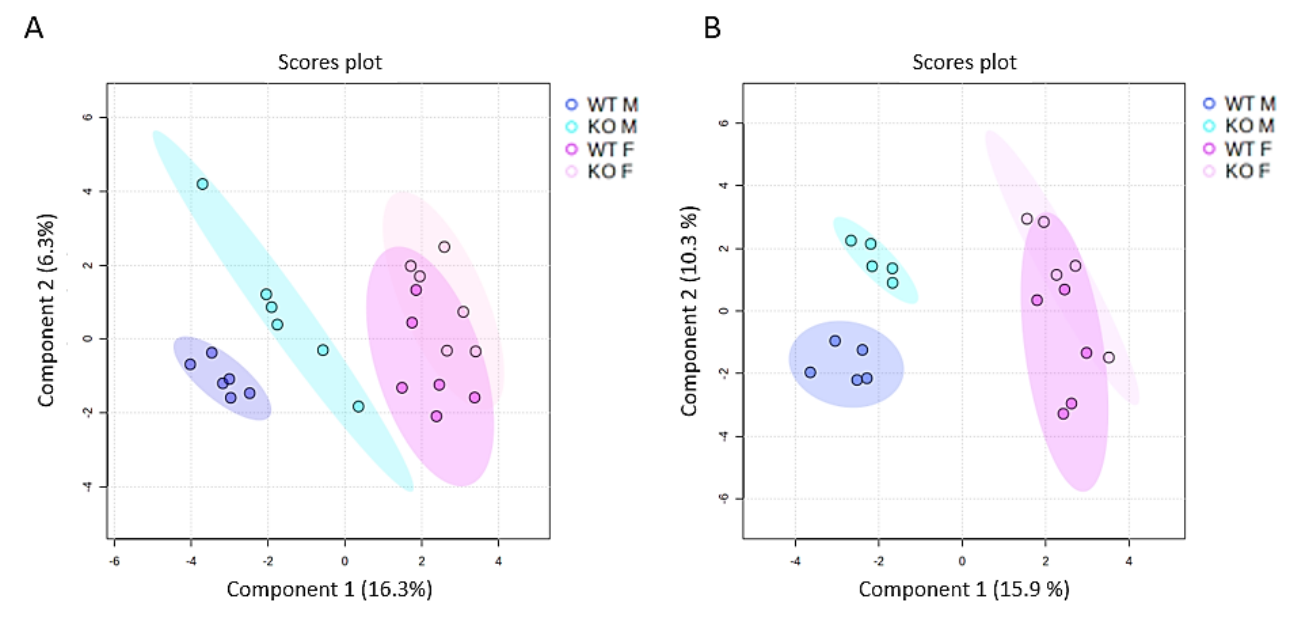


Figure 9. PLS-DA scores plot (A) 4 months and (B) 14 months, created using the Metaboanalyst 6.0 software. Ellipses represent 95 % confidence intervals for each individual group. N = 5 samples per group.

ples from both age groups to further analyse the effects of sex and Sirt3 deficiency (**Figure 9**). In both age groups, samples were distinctively clustered, although there was overlap between WT and KO females. In addition, males and females were clearly separated, especially in 14 month old mice (**Figure 9B**).

The metabolites that contributed most to the separation of the groups in 4 and 14 month old mice were selected based on the VIP scores from the PLS-DA analysis. Metabolites with VIP > 1.5 were selected for further analysis (**Figure 10**).

PLS-DA analysis identified eight metabolites that contributed most to group separation in 4 month old

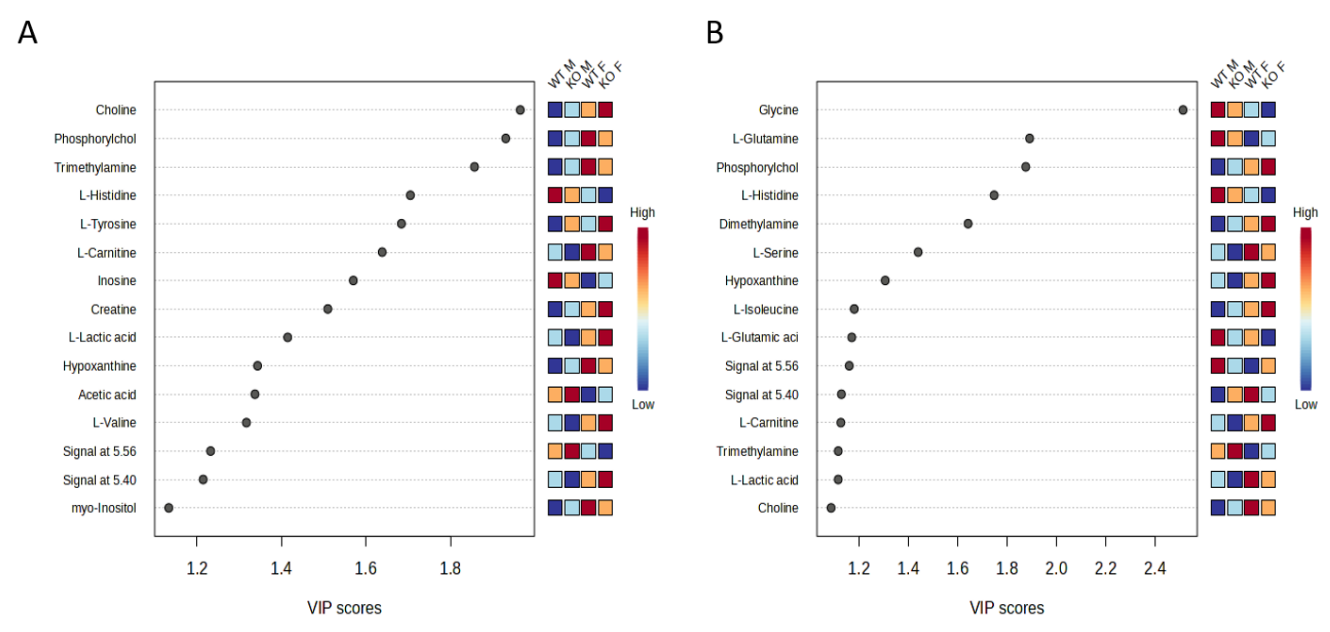


Figure 10. VIP Scores Plot showing the main predictor variables for Sirt3 genotype and sex in kidney tissue of mice at (A) 4 months and (B) 14 months of age. The main predictor variables in 4 month old mice were choline, phosphorylcholine, trimethylamine, L-histidine, L-tyrosine, L-carnitine, inosine and creatine. The main predictor variables in 14 month old mice were glycine, L-glutamine, phosphorylcholine, L-histidine and dimethylamine.

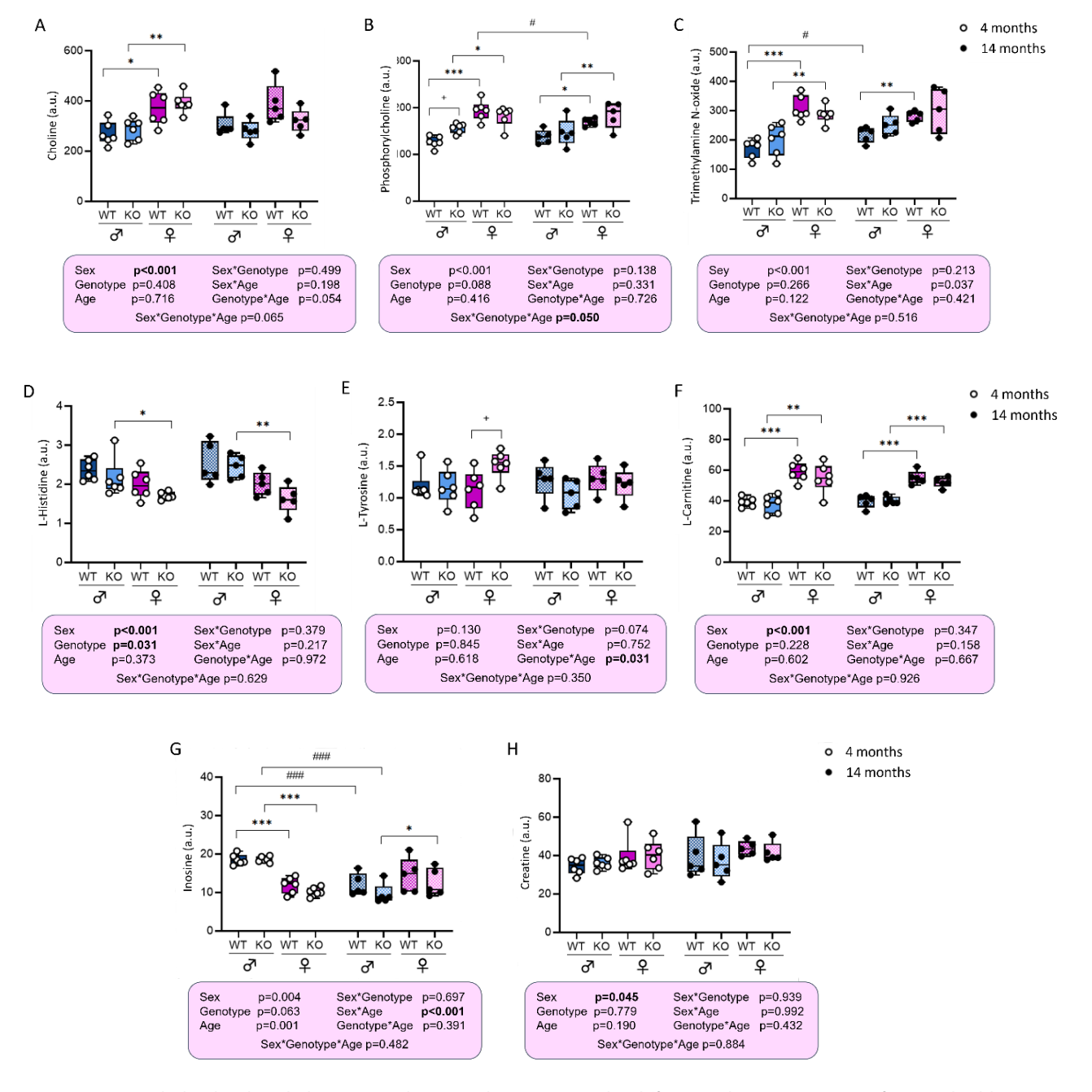


Figure 11. Metabolite levels in kidney tissue that contribute most to the differences between groups of 4 month old mice. (A) choline, (B) phosphorylcholine, (C) trimethylamine-N-oxide, (D) L-histidine, (E) L-tyrosine, (F) L-carnitine, (G) inosine, (H) creatine. A three-way ANOVA was used to analyse the interaction effect of sex, genotype and age. Simple pairwise comparisons were tested using the Bonferroni correction. $^+p<0.05$, WT vs. KO, $^{***}p<0.001$, $^**p<0.05$, males vs. females, $^{##}p<0.001$, $^*p<0.05$, mice aged 4 months vs. 14 months. Metabolite concentrations are expressed in arbitrary units (a.u.). Data are shown as mean \pm SD. N=5-6 samples per group.

mice: choline, phosphorylcholine, trimethylamine, L-histidine, L-tyrosine, L-carnitine, inosine and creatine (**Figure 10A**). Five such metabolites were identified in 14 month old mice: glycine, L-glutamine, phosphorylcholine, L-histidine and dimethylamine (**Figure 10B**). The concentrations of selected metabolites were then analysed using three-way ANOVA to determine the effects of Sirt3 deficiency (genotype), sex and age of the mice (**Figures 11 and 12**).

In 4 month old mice, males generally show decreased concentrations of choline (**Figure 11A**), phosphorylcholine (**Figure 11B**), trimethylamine N-oxide (**Figure 11C**) and L-carnitine (**Figure 11F**) and a higher concentration of inosine (**Figure 11G**). Decreased concentrations of phosphorylcholine and L-carnitine were also observed in older males. In contrast, only KO females of both age groups showed decreased concentrations of L-histidine

(**Figure 11D**). It was also observed that aging generally leads to a decrease in inosine concentrations in males (**Figure 11G**) and an interaction effect of sex and age was observed. In 4 month old mice, females show lower concentrations compared to males, while in 14 month old mice the situation is reversed and females show increased concentrations of inosine.

In 14 month old mice, males generally show decreased concentrations of phosphorylcholine (**Figure 11B**) and increased concentrations of glycine (**Figure 12A**) and L-glutamine (**Figure 12B**). Decreased concentrations of dimethylamine were observed in both young and aged WT males. In addition, aging was observed to lead to an increase in L-glutamine concentrations in males (**Figure 12B**).

A detailed study of survival characteristics between the sexes in relation to Sirt3 has not yet been performed. In this study, we demonstrated a sex-specific effect of Sirt3 on lifespan, with Sirt3 KO males exhibiting a shorter lifespan than WT males, suggesting a greater reliance on Sirt3 for longevity.

Moreover, our results indicated that males rely more on the protective role of Sirt3, which led us to hypothesize that, contrary to males, ovarian hormones may compensate for the lack of Sirt3 in females. The higher expression of Sirt3 in WT males leads to greater dependence and vulnerability in its absence, which is reflected in the shorter lifespan of KO males. Previous research shows significant sex differences in mice following a high-fat diet, suggesting a differential role of Sirt3 in males and females under conditions of nutritional stress, with

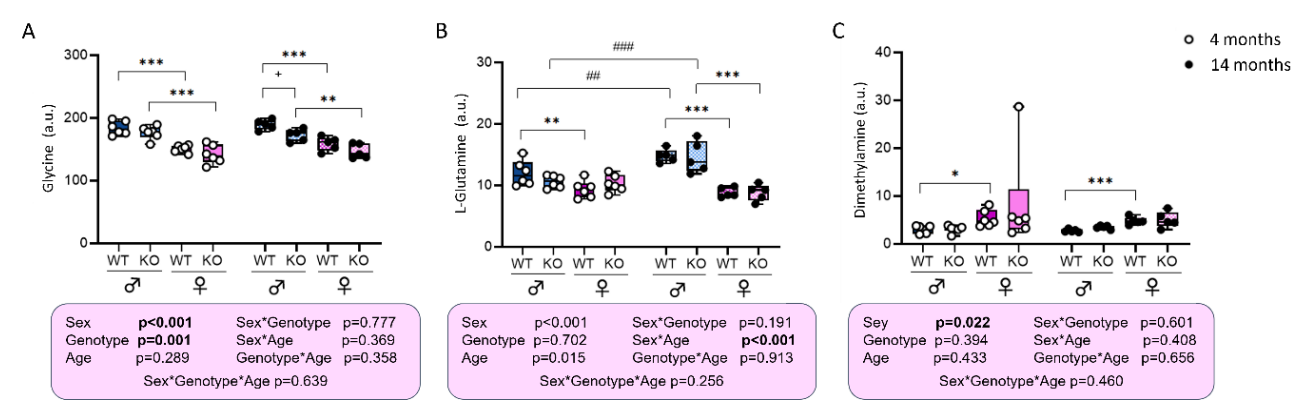


Figure 12. Concentrations of metabolites in the kidney that contribute most to the differences between groups of 14 month old mice. (A) glycine, (B) L-glutamine, (C) dimethylamine. A three-way ANOVA was used to examine the interaction effect of sex, genotype and age. Simple pairwise comparisons were tested using the Bonferroni correction. $^+p<0.05$, WT vs. KO, $^{***}p<0.001$, $^*p<0.01$, $^*p<0.05$, males vs. females, $^{##}p<0.001$, $^{#}p<0.01$, mice aged 4 months vs. 14 months. Metabolite concentrations are expressed in arbitrary units (a.u.). Data are shown as mean \pm SD. N=5-6 samples per group.

Discussion

The aim of this study was to investigate the role of Sirt3 in sex-specific changes in energy homeostasis during aging in mouse kidney. Since the kidneys play a crucial role in maintaining metabolic balance and energy homeostasis it is important to take sex differences into account as they provide a foundation for further studies aimed at therapies for renal diseases. Research shows the importance of Sirt3 in the observed sex-differences in renal disease in mice¹⁵, and our previous results show tissue specific responses and sex-related variations in the interplay of Sirt3, oxidative stress and antioxidative responses in 4 month old mice¹⁶.

males relying more on the protective effect of Sirt3 against HFD-induced metabolic dysregulation¹⁷. It is possible that the protection of females against metabolic dysregulation is due to the complementary action of Sirt3 and female sex hormones. In addition, another study shows sex-specific differences in Sirt3 KO mouse embryonic fibroblasts (MEFs) in response to etoposide treatment¹⁸. Since sex-specific responses to treatment were observed both *in vitro* and *in vivo*, conclusions about the causes of sex-dependent responses must be drawn with great caution.

In humans, epidemiological studies suggest sexspecific differences in kidney function and the rate of its decline. However, discrepancies in the pathophysiology of kidney diseases between men and women are influenced by numerous factors–including age, hormonal status, comorbidities, and access to care–all of which highlight the complexity of interpreting these findings¹⁹.

Men tend to experience a faster age-related decline in kidney function compared to women, contributing to their higher risk of progressing to kidney failure, cardiovascular complications, and overall mortality¹⁹⁻²¹. Our findings in mice model support this observation by revealing a male-specific dependence on Sirt3 for maintaining mitochondrial function and metabolic homeostasis in the kidney. The more pronounced mitochondrial and metabolic dysregulations observed in male mice lacking Sirt3 may offer valuable mechanistic insights into better understanding of increased susceptibility of men to age-related kidney function decline. These insights may help guide future translational studies aimed at identifying sex-specific risk factors and therapeutic targets as our results highlight the importance of considering biological sex in experimental design and interpretation within nephrology research.

Since enzymes involved in oxidative protection are known targets of Sirt3, lipid peroxidation and protein carbonylation were measured to analyse the extent of oxidative damage. Surprisingly, the KO of Sirt3 does not lead to an increased concentration of lipid peroxides in the kidney, but a clear trend towards reduced lipid peroxidation is observed in male mice, both in young and older mice. On the other hand, protein carbonylation levels are higher in young KO females than in WT mice and an interaction effect between genotype and age is observed. In contrast to young mice, old mice show a trend towards lower carbonylation in KOs. Research has shown that the expression of Sirt3 is downregulated during aging²², which would explain the reversal of the trend in oxidative tissue damage in aged mice. However, our analysis does not indicate reduction of Sirt3 expression with aging. To investigate the effects of the loss of Sirt3 on antioxidant enzymes, the activities of CuZnSOD, MnSOD and catalase were also measured. Catalase activity shows a clear trend towards downregulation in females of both age groups, while no change in activity is observed for CuZnSOD and MnSOD. In females of both age groups, a trend towards reduced expression of the master regulator of mitochondrial biogenesis and energy metabolism, PGC-1α, was observed. This was particularly pronounced in KO females. Low expression of PGC-1 α is associated with impaired

mitochondrial function, reduced oxidative phosphorylation and increased susceptibility to oxidative stress²³. This often indicates a decline in cellular energy production and metabolic flexibility, which may contribute to various pathological conditions, including metabolic disorders, neurodegenerative diseases, cardiovascular disease and aging. Since our results do not show increased oxidative damage in females, it is possible that they have compensatory mechanisms for antioxidant protection. Overall, further experiments are needed to draw conclusions on the sex-specific effects of Sirt3 loss on antioxidant enzyme activities and oxidative tissue damage.

Metabolome profiling of kidney tissue was performed to gain insight into sex-specific metabolic changes in KO mice during aging. PLS-DA analysis showed a clear clustering of samples, especially in the group of older mice. Males and females showed distinct clustering patterns, indicating their inherent differences in metabolism. Interestingly, WT and KO males show different cluster patterns, while in females the groups overlap in both age groups. This suggests that the loss of Sirt3 has a greater impact in males than in females, which are metabolically more similar to WT. Greater impact of Sirt3 loss in males is confirmed by survival analysis, which indicates that KO males have shortened lifespan compared to WT.

In young mice, males generally have lower concentrations of creatine, phosphorylcholine, trimethylamine-N-oxide and L-carnitine and higher concentrations of inosine than females. Lower concentrations of these metabolites could indicate mitochondrial dysfunction, impaired energy metabolism and oxidative stress, possibly caused by kidney dysfunction or systemic metabolic stress. Low Lcarnitine levels and reduced expression of HADHB in males indicate impaired fatty acid metabolism. L-carnitine plays a crucial role in fatty acid transport into the mitochondria and HADHB is a mitochondrial enzyme responsible for β-oxidation. Similarly, another research shows that L-carnitine reinforced the mitochondrial β-oxidation and the activity of ROSscavenging enzymes²⁴. On the other hand, these results also suggest that females in general rely more on fatty acid oxidation for energy production. This is in accordance with another research performed on mice, where they show that females have a greater ability to mobilize and utilize fatty acids for energy²⁵. Additional studies focussing on liver metabolomics could provide insights into potential problems in glucose metabolism and further elucidate the changes in fatty acid metabolism. Metabolomic profiles in aged mice also indicate changes in energy metabolism, mitochondrial dysfunction and oxidative stress, but the differences in metabolite levels are less pronounced. Another study found a dysregulation of mitochondrial and immune processes in aging kidney and identified estrogen-related receptors as important modulators of age-related mitochondrial dysfunction²⁶. Even though this study does not take sex-differences into account, modulation of mitochondrial dysfunction through estrogen-related receptors points to possible source of observed sexdifferences in our results. In addition, higher glycine and L-glutamine levels in males indicate changes in amino acid metabolism in response to oxidative stress. It is known that mammalian cells in stress conditions can redirect amino acid metabolism to enable essential processes such as energy production, repair of damaged proteins and combating oxidative stress²⁷. Furthermore, elevated levels of these amino acids may reflect age-related metabolic and mitochondrial dysfunction, but further studies could investigate the interplay between these metabolites and aging processes.

Conclusion

The study highlights the sex-specific role of Sirt3 in the regulation of mitochondrial function, energy metabolism and oxidative stress in murine kidney, with male mice showing a greater dependence on Sirt3 for metabolic homeostasis. Higher Sirt3 expression in male WT mice results in increased susceptibility to Sirt3 deficiency, as evidenced by shorter lifespan of male KO mice. This is also supported by marked metabolomic clustering in male KO mice, indicating substantial metabolic perturbations. Male-specific reductions in metabolites such as creatine, phosphorylcholine, trimethylamine-N-oxide and L-carnitine as well as decreased HADHB expression indicate impaired fatty acid metabolism and mitochondrial dysfunction.

Interestingly, the patterns of oxidative damage differ by sex and age. While young KO females exhibit higher protein carbonylation, old KO mice show reverse trends in oxidative damage, which may berelated to the age-dependent decline in Sirt3 expression observed in previous studies but not confirmed in this analysis. In addition, higher glycine and glutamine levels in males suggest age-related adaptations in amino acid metabolism in response to oxidative stress. The data also indicate that fe-

males rely more heavily on fatty acid oxidation for energy production, which is a potential metabolic advantage under stress conditions. Overall, these results emphasise the need for further studies to investigate sex-specific compensatory mechanisms, the interplay of mitochondrial and metabolic dysfunction and the progression of oxidative damage with aging, particularly in relation to the loss of Sirt3.

Acknowledgements

The authors would like to thank Iva Pesun Medjimorec for her excellent technical assistance.

References

- López-Otín, C., Blasco, M. A., Partridge, L., Serrano, M. & Kroemer, G. Hallmarks of aging: An expanding universe. *Cell* 186, 243–278 (2023).
- 2. Alberts, S. C. et al. The Male-Female Health-Survival Paradox: A Comparative Perspective on Sex Differences in Aging and Mortality. in Sociality, Hierarchy, Health: Comparative Biodemography: A Collection of Papers. (2014).
- 3. Michan, S. & Sinclair, D. Sirtuins in mammals: Insights into their biological function. *Biochem J* **404**, 1–13 (2007).
- 4. Ahn, B. H. *et al.* A role for the mitochondrial deacetylase Sirt3 in regulating energy homeostasis. *Proc Natl Acad Sci U S A* **105**, 14447–14452 (2008).
- 5. Trinh, D., Al Halabi, L., Brar, H., Kametani, M. & Nash, J. E. The role of SIRT3 in homeostasis and cellular health. *Front Cell Neurosci* **18**, 1434459 (2024).
- Chen, Y. et al. Tumour suppressor SIRT3 deacetylates and activates manganese superoxide dismutase to scavenge ROS. EMBO Rep 12, 534–541 (2011).
- Doke, T. & Susztak, K. The multifaceted role of kidney tubule mitochondrial dysfunction in kidney disease development. *Trends Cell Biol* 32, 841–853 (2022).
- 8. Morigi, M., Perico, L. & Benigni, A. Sirtuins in Renal Health and Disease. *J. Am. Soc. Nephrol.* **7**, 1799–1809 (2018).
- 9. Morigi, M. *et al.* Sirtuin 3-dependent mitochondrial dynamic improvements protect against acute kidney injury. *J. Clin. Invest.* **125**, 715–726 (2015).
- 10. Zhang, Y. et al. Sirtuin 3 regulates mitochondrial protein acetylation and metabolism in tubular epithelial cells during renal fibrosis. *Cell Death Dis* **12**, (2021).
- 11. Aebi, H. Catalase in vitro. *Methods Enzymol* **105**, 121–126 (1984).
- 12. Veselkov, K. A. *et al.* Recursive segment-wise peak alignment of biological 1H NMR spectra for improved metabolic biomarker recovery. *Anal Chem* **81**, 56–66 (2009).

- Dieterle, F., Ross, A. & Senn, H. Probabilistic Quotient Normalization as Robust method to aacount for dilution of complex biuological mixtures. *Anal. chem.* 78, 4281–4290 (2006).
- 14. Wishart, D. S. *et al.* NMR and Metabolomics A Roadmap for the Future. *Metabolites* **12**, 1–20 (2022).
- 15. Shen, H. *et al.* Sirtuin-3 mediates sex differences in kidney ischemia-reperfusion injury. *Transl. Res.* **235**, 15–31 (2021).
- Beluzic, R. et al. Sex-Related Differences in Oxidant and Antioxidant Profiles of Murine Kidney and Brain: A Focus on Sirt3-Mediated Regulation. Period Biol 125, (2024).
- 17. Pinteric, M. *et al.* Chronic high fat diet intake impairs hepatic metabolic parameters in ovariectomized Sirt3 KO mice. *Int J Mol Sci* **22**, (2021).
- 18. Simunic, E. *et al.* Sirtuin 3 drives sex-specific responses to age-related changes in mouse embryonic fibroblasts. *Mech Ageing Dev* **222**, 111996 (2024).
- Chesnaye, N. C., Carrero, J. J., Hecking, M. & Jager, K. J. Differences in the epidemiology, management and outcomes of kidney disease in men and women. *Nature Reviews Nephrology* vol. 20 7–20 Preprint at https://doi.org/10.1038/s41581-023-00784-z (2024).
- 20. Neugarten, J., Acharya, A. & Sillbiger, S. R. Effect of Gender on the Progression of Nondiabetic Renal Disease. *Journal of the American Society of Nephrology* **11**, 319–329 (2000).

- 21. Melsom, T. *et al.* Sex Differences in Age-Related Loss of Kidney Function. *Journal of the American Society of Nephrology* **33**, 1891–1902 (2022).
- Xie, S. et al. Activating Mitochondrial Sirtuin 3 in Chondrocytes Alleviates Aging-Induced Fibrocartilage Layer Degeneration and Promotes Healing of Degenerative Rotator Cuff Injury. Am. J. Pathol. 193, 939–949 (2023).
- 23. Abu Shelbayeh, O., Arroum, T., Morris, S. & Busch, K. B. PGC-1α Is a Master Regulator of Mitochondrial Lifecycle and ROS Stress Response. *Antioxidants* **12**, 1075 (2023).
- 24. Ishikawa, H. *et al.* L-carnitine prevents progression of non-alcoholic steatohepatitis in a mouse model with upregulation of mitochondrial pathway. *PLoS One* **9**, e100627 (2014).
- 25. Holcomb, L. E., Rowe, P., O'Neill, C. C., DeWitt, E. A. & Kolwicz, S. C. Sex differences in endurance exercise capacity and skeletal muscle lipid metabolism in mice. *Physiol Rep* **10**, e15174 (2022).
- Wang, X. X. et al. Estrogen-Related Receptor Agonism Reverses Mitochondrial Dysfunction and Inflammation in the Aging Kidney. Am. J. Pathol. 193, 1969–1987 (2023).
- 27. Bröer, S. & Bröer, A. Amino acid homeostasis and signalling in mammalian cells and organisms. *Biochem. J.* **474**, 1935–1963 (2017).